ANALYSIS OF A HIGH TEMPERATURE THERMOSYPHON

André Felippe Vieira da Cunha
Federal University of Santa Catarina
Department of Mechanical Engineering
Solar Energy Laboralory
Florianópolis, Santa Catarina, CEP 88040-900
andre@labsolar.ufsc.br

Márcia B. H. Mantelli
marcia@emc.ufsc.br

Abstract. *High temperature heat pipes represent a new technology under development in Brazil, aiming heat regeneration application in petroleum plants. This paper presents the state of the art of a study conducted in the Mechanical Engineering Department of the Federal University of Santa Catarina. A description of the main characteristics of a high temperature heat pipe is presented, highlighting the material limitations and the selection of the fluid. The thermodynamic behavior of the working fluid is analyzed. A steady state analytical model, which was solved by means of a numerical iterative method, is presented to determine important parameters for the design of high temperature heat pipes, including temperature levels and heat transfer coefficients for the condenser and evaporator. Some preliminary results are presented.*

Keywords*: Heat Pipe, Thermosyphon, Liquid Metal*

1. Introduction

With the world energy crisis, where petroleum become more expensive and scarce, where hydroelectric resources are exhausting and where new technologies that enable the use of solar and eolic energies are not economically viable, the importance of procedures to improve the energetic efficiency of industrial processes is growing, leading to the development of new solutions. High temperature streams (above 600^{o} C), released to atmosphere from furnaces, represent good examples of recoverable thermal energy, available in many plants. In this paper, the technology of high-temperature thermosyphon is considered to be applied in regenerative heat exchangers in petroleum plants.

Thermosyphons are devices with high thermal conductivity that can transfer high quantities of heat. In its most simple form, a thermosyphon is a hollow evacuated metal pipe, charged by a pre-determined amount of an appropriate working fluid. It can be divided into three main sections: evaporator, where the heat is delivered to the device, an adiabatic section (which can or can not exist) and a condenser, where the heat is released. The working fluid located in the evaporator evaporates and, by means of pressure gradients, go toward the condenser region, where it condenses, returning to the evaporator by means of gravity.

A description of high temperature heat pipes can be found in Faghri (1995) and Dunn and Reay (1982). Storey (2003) and Reed (1987) present a numerical and analytical model, respectively, for thermosyphons. In the present work, a different model is introduced, which is solved by means of a numerical iterative method and it is based in the film condensation hypothesis for the condensation and evaporator boiling.

2. High temperature thermosyphon

High temperature thermosyphons work at temperatures above 600^{o}C. The working fluid consists of a liquid metal such as sodium, lithium or potassium. The tube material (metal) must be chemically compatible with the working fluid, to avoid chemical reactions, which could produce undesirable non condensing-gases. The material of the tubes must also resist to the corrosion, while it keeps its mechanical properties at the high working temperatures. The manufacture of this device is also challenging and demands careful, well determined procedures.

2.1. Material mechanical limits

Thermosyphons for operation at temperatures above about 1100 K are typically constructed with refractory metals such as tungsten, molybdenum and some special steel. The use of these materials is not a restriction for applications in space where the environment is at high vacuum and where material and fabrication costs do not constitute a severe constraint. However, for high temperature terrestrial applications the operation environment is usually highly oxidizing or otherwise corrosive and costs are the dominant consideration.

One of the main concerns about the technology of high temperature heat recovery equipments is related to the temperature working limits of the materials used in heat exchangers. Heat exchangers made of stainless steel, for example, can not exceed 700 ^{o}C. When subjected to high temperatures, all metallic alloys get weaker and decrease their stiffness. Consequently, the tubes made of this material are limited to applications where they are subjected to small pressure differences. Figure 1 shows the operation limits of materials that are in current use in heat exchangers. An

alternative approach is to construct thermosyphons made of ceramic tubing, when full advantage can be taken of the high temperature strength and of the excellent corrosion and erosion resistances of selected ceramic materials, including silicon carbide and alumina.

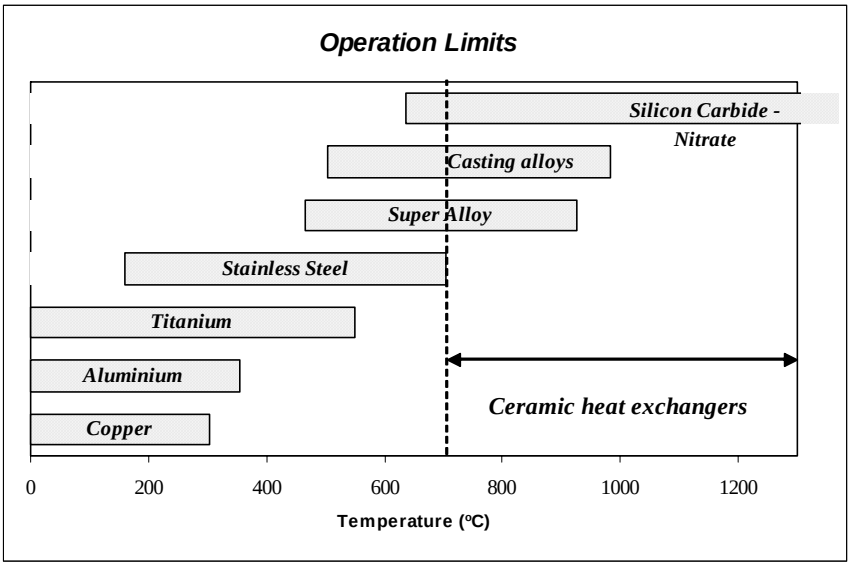

Figure 1. Operation limit of materials in heat exchangers

2.2. Working fluids

The operation fluid used in the thermosyphons must be selected to match the operation temperature range of interest. For high temperature thermosyphons, the usual working fluids are liquid metal including potassium, sodium or lithium. Table 1 shows the melting and boiling points, and the usual range of operation of some liquid metals.

These liquid metals are excellent for heat transfer, having a high conductivity, high heats of vaporization, and a good surface tension coefficient. However, in general they are not compatible with ceramic materials. A ceramic pipe is therefore provided with a protective inner liner which matches the ceramic expansion characteristics. Stainless steel and Inconel are materials appropriate to be used with these working fluids.

Table 1. Melting and boiling points of liquid metals at atmosphere pressure (1 atm).

Working Fluids	Melting Point	Boiling Point	Usual Range
Sodium	98 ^{o}C	892 ^{o}C	600 up to 1200 ^{o}C
Lithium	179 ^{o}C	1340 ^{o}C	1000 up to 1800 ^{o}C
Potassium	62 ^{o}C	774 ^{o}C	500 up to 1000 ^{o}C
Mercury	-39 ^{o}C	357 ^{o}C	

Sodium, potassium and lithium are elements that require careful handling because they are highly reactive with water and humidity, liberating flammable gases. Potassium reacts with water and humidity to form explosive mixtures with air at normal temperature, for example.

Yamamoto et al. (1994) analyzed experimentally heat pipes with mercury as a working fluid. Despite presenting good thermal performance, mercury is a highly toxic substance and has been avoided in thermosyphons for industrial applications. They are, however, considered a reasonable option for academic study purposes.

2.3. Thermodynamic of sodium thermosyphon

The transient behavior of a high-temperature thermosyphon with a liquid metal has been analyzed. The working fluid selected for the present study is sodium. Sodium is solid at ambient temperature. When heat is applied to the evaporator, sodium melts or sublimates. From sodium saturation properties of liquid and vapor (see Fink, 1995) it is observed that, due to its low vapor pressure level, the sodium does not sublimate, going first through melting and after the complete melting, through evaporation.

To know whether sodium in its vapor, liquid and solid states can be found simultaneously during the melting process is of primary importance for modeling purposes. Therefore, a one-dimensional steady state conduction heat transfer study for sodium cylinder was performed. The diameter of the cylinder was considered as 22 mm, with a 220 m of length. A 600 kW/m^2 heat flux was considered applied to the external surface, resulting in a temperature gradient of about 145 ^{o}C. As this temperature is smaller than the temperature difference between the melting and evaporation points, one can conclude that the sodium will melt completely before the evaporation process starts. Therefore, the amount of vapor above the surface of sodium in the solid sate and during the melting processes is considered negligible.

Figure 2 represents a diagram of the pressure as a function of the specific volume of sodium. Point "*a*" is considered as the starting point, when heat is applied to solid sodium inside the thermosyphon. All the melting process happens between the points "*a*" and "*d*", at a constant pressure level. The pressure increases up to the point "*e*", as vapor starts to be formed and occupies all the remaining volume of the thermosyphon. The resulting specific volume remains constant for the thermosyphon operation conditions.

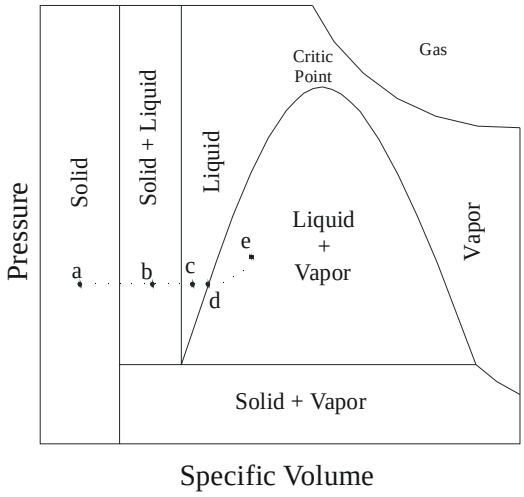

Figure 2. Pressure-specific volume diagram of sodium

3. Proposed model

A model is proposed with the objective of giving insight in the performance of high-temperature thermosyphons. In the model, the thermosyphon is divided into three regions: evaporator, condenser and adiabatic section. The evaporator and adiabatic section are subdivided into two volumes: the region of liquid film and the vapor nucleus. The region of evaporator contains these two volumes plus a liquid pool. The effect of non-condensing gases is considered too. Steady-state and uniform temperature distributions within the wall of the evaporator and condenser (lumped formulation) are considered.

3.1. Condenser

The liquid film over the vertical tube wall inside the pipe as considered a plain vertical surface and the condensation model of Nusselt (Nusselt apude Incropera, 2002) over vertical surfaces is considered. Based on the well known Nusselt theory, the velocity u is given by the expression:

$$u(y) = \frac{g(\rho_l - \rho_v)\delta^2}{\mu_l}\left[\frac{y}{\delta} - \frac{1}{2}\left(\frac{y}{\delta}\right)^2\right], \tag{1}$$

where g is the gravitational acceleration, ρ_l is the mass density of liquid, ρ_v is the mass density of vapor, μ_l is the dynamic viscosity of liquid and y is the horizontal distance to the wall. The film thickness $\delta(x)$ is given by:

$$\delta(x) = \left[\frac{4k_l\mu_l(T_{sat} - T_w)x}{g\rho_l(\rho_l - \rho_v)h_{lv}}\right]^{1/4}, \tag{2}$$

where k_l is the thermal conductivity, T_{sat} is the temperature of saturation, T_w is the temperature of wall, h_{lv} is the latent heat of vaporization and x is the axial distance between the top of film liquid and the condenser bottom.

The mean film heat transfer coefficient $\bar{h}_L$ is determined using the expression:

$$\bar{h}_L = \frac{1}{L_c}\int_0^{L_c} h\,dx \longrightarrow \bar{h}_L = 0,943\left[\frac{\rho_l g(\rho_l-\rho_v)h_{lv}^{'}k_l^3}{\mu_l(T_{sat}-T_w)L_c}\right]^{1/4}, \tag{3}$$

where $h_{lv}^{'} = h_{lv} + 0,68\,Cp_l\,(T_{sat}-T_w)$, Cp_l is the specific heat of liquid and L_c is the length of condenser. This $h_{lv}^{'}$ expression was suggested by Rohsenow (apude Incropera, 2002) due to subcooling of the film.

Finally the mass flow rate of liquid leaving the condenser, $\dot{m}_{lc}$, is given by:

$$\dot{m}_{lc} = \frac{2\pi\rho_l g(\rho_l-\rho_v)\delta_{L_c}^3}{\mu_l}\left[\frac{r_i}{3}-\frac{5\delta_{L_c}}{24}\right], \tag{4}$$

where δ_{Lc} is the film thickness at the end of condenser and r_i is the inside tube radius.

The vapor located both in the condenser and in the evaporator is considered saturated. The properties of the liquid are evaluated at the average temperature between the wall and the vapor.

3.2. Adiabatic section

In the adiabatic section, the equations derived from the Nusselt analysis can not be applied, because there is no radial heat transfer and the axial heat conduction is relatively small. One of main factors causing low axial conduction is the small thickness and the low thermal conductivity material of the wall. The thickness of the liquid film is considered constant in this region

3.3. Evaporator

In the evaporator section, the temperature level of vapor is considered smaller than the temperature of the wall. The film thickness $\delta_{La+Lc+\Delta x}$ and the mean film heat transfer coefficient $\bar{h}_{ef}$ are calculated using Nusselt's model of condensation at a plain vertical surface, given by the following equations, respectively:

$$\delta_{L_a+L_c+\Delta x} = \left[\delta_{L_a+L_c}^4 + \frac{4k_l\mu_l(T_{sat}-T_w)(x-L_a-L_c)}{g\rho_l(\rho_l-\rho_v)h_{lv}}\right]^{1/4}, \tag{5}$$

where L_a is the length of adiabatic section, L_c is the length of condenser and δ_{La+Lc} is the film thickness at the end of the adiabatic section, and:

$$\bar{h}_{ef} = \frac{g\rho_l(\rho_l-\rho_v)h_{lv}}{3\mu_l(T_v-T_w)(L_e-L_p)}\left[\left(C_1(L_t-L_p)+\delta_{L_c+L_a}^4 - C_1(L_c+L_a)\right)^{3/4} - \delta_{Lc+L_a}^3\right], \tag{6}$$

where $C_1 = 4k_l\mu_l(T_{sat}-T_w)/g\rho_l(\rho_l-\rho_v)h_{lv}$.

In the region of the liquid pool, nucleate boiling is considered. Some correlations of the pool mean heat transfer coefficient have been obtained in the literature such as that of Shiraishi et. al (Shiraishi et. al apude Ong 2003), given by:

$$\bar{h}_{ep} = 0,32\left[\frac{\rho_l^{0,65}k_l^{0,3}c_{pl}^{0,7}g^{0,2}}{\rho_v^{0,25}h_{lv}^{0,4}\mu_l^{0,1}}\right]\left(\frac{P_{sat}}{P_{atm}}\right)^{0,23} q_e^{0,4}, \tag{7}$$

where P_{sat} is the pressure of saturation is P_{atm} the atmosphere pressure is and q_e is the heat flux of evaporator, and the correlation of Rohsenow (Rohsenow apude Noie, 2003), given by:

$$\bar{h}_{ep} = \frac{q_e^{2/3}}{\frac{C_{sf} h_{lv}}{c_{pl}} \left\{ \frac{1}{h_{lv} \mu_l} \left(\frac{\sigma}{g[\rho_l - \rho_v]} \right)^{1/2} \right\}^{0,33} \Pr}, \tag{8}$$

where C_{sf} is the Rohsenow constant obtained from experimental data. Values for C_{sf} were suggested by Pioro (1999) which can be applied for some specific conditions. In Eq. 9, *Pr* is Prandtl Number ($\Pr = Cp\,\mu/k$).

Another useful literature correlation was developed by Shevchuk et al (1999) for sodium, and reads as:

$$\bar{h}_{ep} = 3{,}15\, q_e^{2/3} \tag{9}$$

The average heat transfer coefficient of evaporator is computed as a weighed mean of the heat transfer coefficients of film and pool, as show by Equation (10).

$$\bar{h}_e = \frac{\bar{h}_{ep} L_p + \bar{h}_{ef} L_f}{L_e} \quad , \tag{10}$$

where L_f is the film length of evaporator ($L_f = L_e - L_p$) and L_p is the pool length..

3.4. Non-condensing gases region

The present model also considers the non-condensing gases present inside the thermosyphon, after vacuum is obtained. These gases are clustered in the upper part of the pipe during operation, decreasing the effective length of the thermosyphon. The heat transfer coefficient in the presence of non-condensing gases is significantly smaller compared to the remaining region where condensation takes place. In this work, this region is considered adiabatic because these gases disturb the heat transfer process within the region they reside.

Knowing the temperature and pressure of the thermosyphon after the vacuum is established, it is possible to determine the mass and volume of non-condensing gases through the Ideal Gases Law (*PV=nRT*). Therefore, the effective length of condenser can be calculated for the operation conditions of the thermosyphon. The pressure of non-condensing gases is considered the same of the pressure of the vapor, while the temperature is obtained from an area weighed mean of the vapor and wall temperatures.

3.5. Flowchart of the model

The model is solved numerically by means of an iterative process, using FORTRAN. The resulting flowchart is showed in Figure 3. The input data for the model are: lengths of condenser (L_c), adiabatic section (L_a) and evaporator (L_e); mass of sodium (*Ms*), external heat transfer coefficient (h_{extc}), condenser external wall temperature (T_{extc}), tube inner diameter (D_i) and heat transfer rate (Q_e).

The first step consists on the estimation of the temperatures of wall and vapor, which must satisfy the heat transfer rate, taking into account the presence of non-condensing gases. The temperature of the vapor it is obtained by small temperature increments (ΔT_v). No calculation is required for the adiabatic section because the thickness of the liquid film is constant and the axial heat transfer is considered negligible.

After determination of the temperatures and of the profile of the liquid film in the condenser region, temperatures of the wall are computed, as well as the profile of the liquid film thickness in the evaporator. The temperature of the wall in contact with the liquid film is obtained in the same way as that of the condenser liquid film. The mass balance is checked in each time step considered, to guarantee that total amount of liquid, including the liquid film and the pool remains constant. The temperature of the vapor in the evaporator region is considered equal to that of the condenser. The heat transfer rate to the pool and the liquid film is considered proportional to the heating area.

For the liquid pool region, the temperature of the wall is a function of the heat transfer coefficient, which in turn is calculated from literature correlations. The temperature of pool is taken as the average of the surface and pool bottom temperatures. The correlation obtained for the sodium saturation temperature and pressure was taken from Fink and Leibowitz (1995). The condenser external heat transfer coefficient (h_{extc}) is taken from the correlation of Churchill and Bernstein (apude Incropera, 2002), if $Re_D Pr > 0.2$, given as:

$$h_{ext.c} = \frac{k}{D_e} \left(0{,}3 + \frac{0{,}62\, \mathrm{Re}_D^{1/2}\, \mathrm{Pr}^{1/3}}{\left[1 + \left(0{,}4/\mathrm{Pr} \right)^{2/3} \right]^{1/4}} \left[1 + \left(\frac{\mathrm{Re}_D}{282000} \right)^{5/8} \right]^{4/5} \right), \tag{11}$$

where D_e is the tube outer diameter and Re_D is the Reynolds number based on the outer diameter.

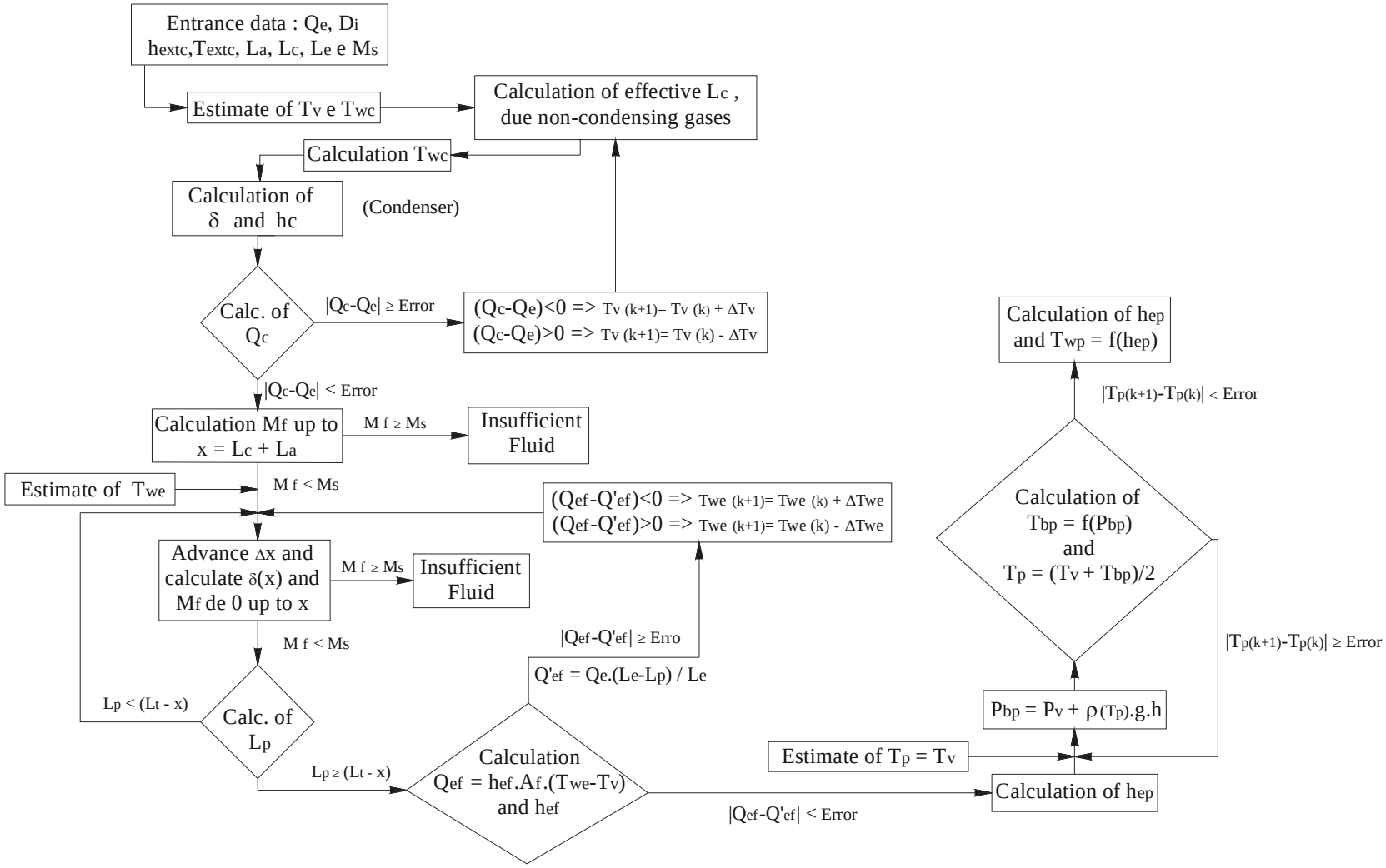

Figure 3. Flowchart of model about high temperature thermosyphon

4. Results

A simulation has been carried out with the input data presented in Table 2. The results of the effective length of thermosyphon, the length of liquid film and the length of pool are 0.97 m, 0.852 m and 0.118 m, respectively. The resulting temperatures obtained using the present model shows a very small variation among the thermosyphon regions, where the temperatures were set about 950 K, as it can be seen in Figure 4.

Table 2. Input data.

Inner diameter (D_i)	0.032 m	Adiabatic section length (L_a)	0.19 m
Outer diameter (D_e)	0.035 m	Outer temperature (condenser)	300 K
Heat transfer rate (Q_e)	2500 W	Outside velocity of air (condenser)	10 m/s
Condenser length (L_c)	0.48 m	Mass of sodium	80 g
Evaporator length (L_e)	0.33 m		

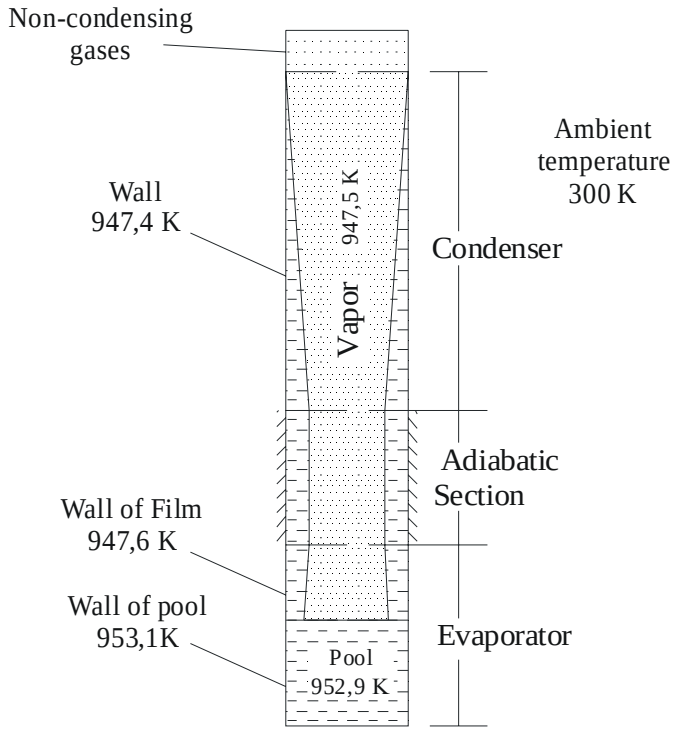

Figure 4. Results of temperature in the thermosyphon.

The computed heat transfer rates, obtained from the correlations presented in Section 3, are show in Table 3. For the condenser region, the heat transfer was calculated from the Nusselt correlation, which is compared with the results of the numerical integration of the local coefficient of convection ($h = k_l / \delta$). For the liquid pool region, the results of the three correlations do not agree among themselves. This large difference shows that these correlations probably can not be applied to a liquid metal such as sodium.

Table 3. Heat transfer coefficients.

Condenser		
Numerical integration of $h = k_l / \delta$	883,944.40 W/m^{2}K	
Nusselt	901,513.80 W/m^{2}K	
Evaporator		
Numerical integration of $h = k_l / \delta$	778,706.50 W/m^{2}K	*Film*
Nusselt	770,593.30 W/m^{2}K	
Shiraishi	21,046.95 W/m^{2}K	*Pool*
Rohsenow	465,941.90 W/m^{2}K	
Shevchuk	5,559.63 W/m^{2}K	

The present model results are also compared with those of the equivalent thermal resistance model (see Brost, 1996). The equivalent thermal resistance model considers steady-state conditions and is based on the analogy between thermal and electric circuits. The input data of Table 2, with the same value for condenser external heat input (77.85 W/m^2K), is used in the thermal circuit model.

The results for the heat transfer rate, the temperature of vapor and the temperature of liquid pool for thermal circuit model are 2704.41 W, 1234.91 K and 1234.87 K, respectively. It is observed that the difference of heat transfer rates and temperature of the vapor is large than obtained in the proposed model, about 8.16% and 30%, respectively, as observed in the Table 4. The use of thermal resistance of wall in Brost's model and the different correlations used for the heat transfer coefficient of the liquid pool can be the major reasons for the difference observed between both models.

Table 4. Results of proposed model and Brost's model.

	Brost's Model	Proposed Model
Temperature of vapor	1234.91 K	947.5 K
Temperature of pool	1234.87 K	952.9 K
Heat transfer rate	2704.41 W	2500 W

5. Conclusions

In this paper, a model is proposed for a high temperature thermosyphon. This model was solved iteratively, using numerical algorithms. The working fluid used for this model is sodium. This model considers steady-state conditions and assumes a uniform (lumped) temperature in the evaporator and condenser walls.

The results of simulations show the necessity of an experimental study in order to generate trustworthy correlations for both evaporator and condenser regions of thermosyphon. The correlations of the literature present great divergence with correlations obtained by Nusselt.

6. References

Brost, O, 1996, "Closed Two-Phase Thermosyphons", Class Notes, IKE, University of Stuttgart, Germany.

Dunn, P. D., and Reay, D. A., 1982, "Heat Pipes", 3rd ed., Pergamon Press, Oxford.

Faghri, A., 1995, "Heat Pipe Science and Technology", Taylor and Francis, Washington.

Fink, J. K., and Leibowitz, L., 1995, "Thermodynamic and Transport Properties of Sodium Liquid and Vapor", Argonne National Laboratory, Reactor Engineering Division.

Incropera, Frank. P. and Witt, David P., 2002, "Fundamentos de Transferência de Calor e de Massa", 5º ed., ed. LTC , Rio de Janeiro, RJ.

Noie, S. H.; Kalaei, M. H. and Khoshnoodi, M., 2003, "Experimental Investigation of a Two Phase Closed Thermosyphon", The 7th International Heat Pipe Symposium, October 12-16, Jeju, Korea.

Ong, K. S., 2003, "A Simple Theoretical Model of a Thermosyphon", The 7th International Heat Pipe Symposium, October 12-16, Jeju, Korea.

Pioro, I. L., 1999, "Experimental evaluation of Constants for the Rohsenow Pool Boiling Correlation", International Journal of Heta Transfer and Mass, vol. 42, pp. 2003-2013.

Reed, J. G. and Tien, C. L., 1987, "Modeling of the Two-Phase Closed Thermosyphon", Transactions of the ASME, vol. 109, August.

Shevchuk, E. N.; Fialko, N. M. and Maletskaya, O. E., 1999, "Research and Estimation of Evaporation Conditions in Solar Receiver of a Sodium Heat Pipe", Proceeding of the 11th International Heat Pipe Conference, Tokyo, Japan.

Storey, J. Kirk, 2003, "Modeling the Transient Response of a Thermosyphon", Ph. D. Thesis, Department of Mechanical Engineering, Brigham Young University, December.

Yamamoto, T.; Nagata, K.; Katsuta, M. and Ikeda, Y., 1994, "Experimental Study of Mercury Heat Pipe", Experimental Thermal and Fluid Science, vol. 9, pp. 39-46.